Path Integral Monte Carlo Simulation of Isotopic Liquid Helium Mixtures

Massimo Boninsegni[1] and David M. Ceperley[1,2]

[1]*National Center for Supercomputing Applications, University of Illinois at Urbana-Champaign, Urbana, Illinois 61801*

[2]*Department of Physics, University of Illinois at Urbana-Champaign, Urbana, Illinois 61801*

(Received 15 November 1994)

We report results of a path integral Monte Carlo simulation of a liquid ^{3}He-^{4}He mixture at low temperature. In the limit of low ^{3}He concentration, a kinetic energy of 17 K is found for the ^{3}He atoms; the ^{3}He effective mass is $m^* = 2.3m$. The restricted path integral Monte Carlo method was utilized to investigate the separation of the mixture into a ^{3}He- and ^{4}He-rich phase.

PACS numbers: 67.60.–g, 61.20.Ja

The phase diagram of liquid mixtures of ^{3}He and ^{4}He has elicited considerable theoretical [1] and experimental [2] interest. At a low ^{3}He concentration, ^{3}He atoms can be regarded [3] as essentially free quasiparticles, with an effective mass m^*. As the concentration x is increased, two important macroscopic effects are observed: the gradual suppression of ^{4}He superfluidity, with the λ point becoming a line $\lambda(x)$ ending at the tricritical point ($x_t = 0.669$, $T_t = 0.872$ K), and, below T_t, the separation of the mixture into two coexisting phases, a ^{4}He- and ^{3}He-rich phase. In the $T \to 0$ limit, ^{4}He is excluded from the ^{3}He-rich phase, whereas the extrapolated solubility of ^{3}He in ^{4}He is finite, around 6.6%.

Microscopic studies of the mixtures, based on *ab initio* interatomic potentials, have so far been limited to a single ^{3}He atom in liquid ^{4}He; ground state estimates for this case have been obtained by means of variational calculations, based on Jastrow-type wave functions [4], possibly with the inclusion of backflow effects [5]. Quantitative discrepancies exist between variational results and experimental data; for instance, the predicted value of the ^{3}He effective mass m^* is about $1.7m$ [5], against an experimental value of $m^* = 2.3m$ [6]. Also, variational calculations predict [4] a kinetic energy of a ^{3}He atom in liquid ^{4}He around 18–19 K; however, recent deep inelastic neutron scattering measurements of the momentum distribution in dilute liquid ^{3}He-^{4}He mixtures at low temperature [7] yielded a kinetic energy of 11 ± 3 K for the ^{3}He atoms, considerably lower than expected. Because the calculations mentioned above are variational, the discrepancies with the experiment could be due to inadequacies of the trial wave functions utilized.

In this Letter we report results of a path integral Monte Carlo (PIMC) study of a ^{3}He-^{4}He mixture; our aim was (a) to obtain reliable low-temperature kinetic energy estimates for a single ^{3}He atom using a technique (PIMC) which, unlike a variational calculation, is exact and needs no *a priori* physical assumption (e.g., a trial wave function); (b) to explore quantitatively the phase diagram of the mixture at finite ^{3}He concentration.

For a single ^{3}He impurity in liquid ^{4}He, we obtain a ground state kinetic energy of 17.1 K, lower than the variational estimate but still significantly higher than the experimental result; we calculated the effective mass m^* of the ^{3}He atom and found it to be about 2.3 times the bare ^{3}He mass, in excellent agreement with experimental findings.

In order to obtain theoretical insight into the phase diagram of the mixture at finite x, we simulated a system with an equal number of ^{3}He and ^{4}He atoms at 250 and 500 mK and observed an equilibrium situation with two distinct phases; the exclusion of ^{4}He atoms from the ^{3}He-rich phase, as the temperature is lowered, is qualitatively reproduced; a well-defined ^{3}He-^{4}He interface is observed at $T = 250$ mK; the calculated equilibrium low-temperature solubilities are in reasonable quantitative agreement with experiment.

In the remainder of this Letter we give a brief description of the technique utilized in our calculation, as well as of the different systems studied, then present the results. We considered a system of N helium particles in a box, with periodic boundary conditions. Of these particles, $n = xN$ are ^{3}He and the remaining $N - n$ are ^{4}He atoms. We used a two-body Aziz potential to model the interaction between helium atoms; this potential affords an accurate description of the energetic and structural properties of liquid helium, including the momentum distribution [8]. The computational technique which we adopted, path integral Monte Carlo, is a powerful tool to calculate finite-temperature properties of quantum many-particle systems. Here we only sketch its essential elements; for a more thorough description, see, for instance, [9]. If we consider a quantum system of N particles, characterized by a Hamiltonian $\hat{H}$, the thermal average of a physical observable $\hat{O}$ at a temperature T is given by

$$\langle \mathcal{O} \rangle = \frac{1}{Z} \int d\mathbf{R}\, \mathcal{O}(\mathbf{R}) \rho(\mathbf{R}, \mathbf{R}; \beta), \qquad (1)$$

where $\beta = 1/k_B T$ and $\mathbf{R} \equiv \{\mathbf{r}_1, \mathbf{r}_2, \ldots, \mathbf{r}_N\}$, $\mathbf{r}_i$ being the coordinate of the ith particle; $\rho(\mathbf{R}, \mathbf{R}; \beta) = \langle \mathbf{R} | e^{-\beta \hat{H}} | \mathbf{R} \rangle$ is the many-body density matrix and $Z = \int d\mathbf{R}\, \rho(\mathbf{R}, \mathbf{R}; \beta)$ is the partition function. A PIMC calculation consists of generating stochastically a set of configurations $\{\mathbf{R}_i\}$, statistically sampled from a probability density proportional to $\rho(\mathbf{R}, \mathbf{R}; \beta)$; the quantity $\langle \mathcal{O} \rangle$ can thus be evaluated by averaging over the set of values $\{\mathcal{O}(\mathbf{R}_i)\}$. Of

 0031-9007/95/74(12)/2288(4)$06.00

course, the explicit form of $\rho(\mathbf{R},\mathbf{R};\beta)$ is not known; however, one can use the identity $e^{-\beta\hat{H}} = (e^{-\tau\hat{H}})^M$, with $\tau = \beta/M$. As $\tau \to 0$, explicit approximations for $\rho(\mathbf{R},\mathbf{R}';\tau)$ can be obtained, making it possible to generate the configuration sample $\{\mathbf{R}_i\}$ by sampling "paths" through the configuration space from a probability density proportional to $\rho(\mathbf{R}_0,\mathbf{R}_1;\tau)\rho(\mathbf{R}_1,\mathbf{R}_2;\tau)\cdots\rho(\mathbf{R}_{M-1},\mathbf{R}_M;\tau)$.

In order to account for particle indistinguishability, the paths must be allowed to close onto a permutation of the initial positions of the N particles, i.e., $\mathbf{R}_M = P\mathbf{R}_0$, P being a permutation of the particle's indices. Permutations become increasingly important at low temperature; thus, a key ingredient of the PIMC method is an algorithm to sample permutations efficiently [9].

A problem arises in the case of fermion systems; the paths closing onto odd permutations of the initial positions yield a negative contribution to the observable average. At low temperatures, contributions of opposite sign cancel almost exactly; thus, the method becomes numerically "noisy," and in practice unusable unless some procedure is sought to include only positive contributions. As one of us has shown [10], it is possible to perform an exact calculation including only even permutations by restricting the paths $\{\mathbf{R}_0,\mathbf{R}_1,\ldots\mathbf{R}_j,\ldots,\mathbf{R}_M\}$ to regions of the configuration space in which the exact many-body density matrix $\rho(\mathbf{R}_0,\mathbf{R}',t) > 0$ for $0 < t < \beta$. In general, the locations of the nodes of the true $\rho(\mathbf{R},\mathbf{R}',t)$ are not known. Thus, in the restricted path integral Monte Carlo (RPIMC) method one uses the nodes of a "trial" density matrix $\rho_T(\mathbf{R},\mathbf{R}',t)$; if the nodes of ρ_T are substantially correct, the method provides accurate thermodynamics for Fermi systems. The RPIMC procedure has been applied to the study of normal liquid ^{3}He [11], using the nodes of a free-particle density matrix; the error in energy due to the restricted-path approximation can be estimated to be less than 0.5 K per atom.

We now turn to our results. We performed PIMC simulations for systems of 54 and 108 particles; we used a pair-product approximation [9] as our high-temperature density matrix $\rho(\mathbf{R},\mathbf{R}',\tau)$, and observed convergence of the numerical estimates with $\tau = 0.025$ K^{-1}. We obtained results for a single ^{3}He particle in bulk ^{4}He and for a finite concentration (around 9%) of ^{3}He atoms, in the temperature range $0.250 \le T \le 2$ K, at the ^{4}He equilibrium density ($\rho_4 = 0.0218$ Å^{-3}). For a single ^{3}He atom the calculation is exact, as one does not need to antisymmetrize; the RPIMC method was adopted to study systems with more than one ^{3}He atom, with nodal regions specified by the noninteracting density matrix. This approximation is very accurate for the low fermion densities which we have considered for the low x part of the calculation, i.e., x below 10%. In Table I we report the results for the ^{3}He kinetic energy; the data show little dependence on x or N, and even the temperature dependence is small, at least below 1 K. If we assume a Landau-Pomeranchuk form [3] for the ^{3}He atom excitation spectrum, we expect the ^{3}He kinetic energy $K_3(T)$ to depend on temperature as $K_3(T) = K_3(0) + \alpha T$. Extrapolation of our data yields $K_3(0) = 17.1 \pm 0.1$ K and $\alpha = 0.8 \pm 0.1$ K^{-1}. A check of the consistency of our kinetic energy data can be obtained by calculating the chemical potential of the single ^{3}He atom at $T = 0$; this can be done by expressing the free energy change due to the replacement of one ^{4}He atom with a ^{3}He one as

TABLE I. ^{3}He kinetic energy (in K), computed by PIMC, for a ^{3}He-^{4}He liquid mixture, at different temperatures and ^{3}He concentrations x. Statistical errors (one standard deviation), in parentheses, are on the last digit.

T (K)	$N = 54$	$N = 108$	x
0.25	17.4(3)	17.5(2)	$1/N$
0.50	18.1(3)	17.5(3)	$1/N$
1.00	17.9(3)	17.7(3)	$1/N$
2.00	-	18.2(4)	$1/N$
1.00	17.7(2)	18.1(2)	0.093
2.00	18.8(1)	18.7(1)	0.093

$$\mu_3 = \mu_4 + \int_{m_3}^{m_4} \frac{dm}{m} K_m , \qquad (2)$$

where μ_4 is the ^{4}He chemical potential, and K_m is the kinetic energy of a helium atom of mass $m_3 < m < m_4$; in deriving (2) we have taken advantage of the fact that the derivative of the free energy with respect to the mass is proportional to the kinetic energy. We estimated the integral in (2) by means of a trapezoidal approximation; for the ^{4}He kinetic energy we used the value 14.3 ± 0.1 K, which we found for pure ^{4}He. We used for μ_4 its experimental value (-7.14 K). We obtain, at $T \to 0$, $\mu_3 = -2.6 \pm 0.2$ K, consistent with the experimental results [12] of about -2.75 K.

To gain further insight into the local environment experienced by a single ^{3}He particle embedded in liquid ^{4}He, one can look at the local ^{4}He density $\rho_{34}(r)$ in the vicinity of the ^{3}He impurity and compare it to the ^{4}He density $\rho_{44}(r)$ in the vicinity of a ^{4}He atom in pure liquid ^{4}He [9]. In Fig. 1 ρ_{34} and ρ_{44} are compared to the corresponding local density ρ_{33} for pure liquid ^{3}He [11] at its equilibrium density ($\rho_3 = 0.016\,355$ Å^{-3}). The data shown in Fig. 1, all at $T = 250$ mK, clearly show how the local density in the vicinity of a single ^{3}He particle in liquid ^{4}He (triangles) is very close to the one in the vicinity of a ^{4}He atom (dashed line), considerably larger than the one in the vicinity of a ^{3}He atom in pure liquid ^{3}He (squares); thus, due to the interaction hard core, the ^{3}He atom experiences a greater localization in liquid ^{4}He, which accounts for the increased kinetic energy.

The disagreement between the experimental result of Ref. [7] and our theoretical estimate is disconcerting, as we believe the latter to be very reliable, owing to the accuracy of the model potential utilized and of the numerical

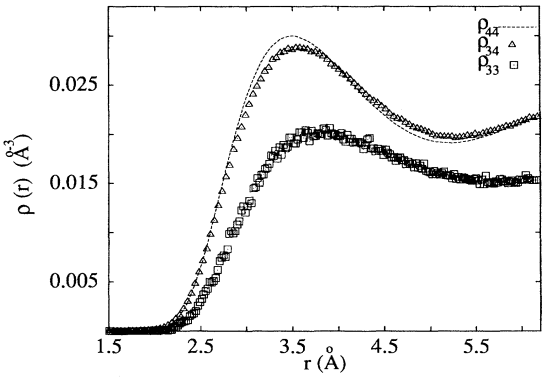

FIG. 1. Dashed line: local density $\rho_{44}(r)$ in the vicinity of a ^{4}He atom in liquid ^{4}He at the equilibrium density. Triangles: local ^{4}He density $\rho_{34}(r)$ in the vicinity of a ^{3}He atom embedded in liquid ^{4}He, at the ^{4}He equilibrium density. Squares: ^{3}He density $\rho_{33}(r)$ in the vicinity of a ^{3}He atom in bulk liquid ^{3}He at the ^{3}He equilibrium density. Statistical errors (one standard deviation) are given by the sizes of symbols; they are not shown for clarity for the dashed line, for which they are of the same size as the triangles. All curves are at $T = 250$ mK.

technique adopted. It is worth mentioning that in a neutron scattering experiment one probes the momentum distribution and infers the value of the kinetic energy from its second moment; such a procedure is quite complicated, and it is conceivable that the kinetic energy estimate could be altered by a variety of factors experimentally hard to control. For instance, as suggested also in Ref. [7], the momentum distribution often features non-Gaussian tails, difficult to detect experimentally but carrying enough weight to affect significantly the estimate of the moments.

Let us now turn to the determination of the effective mass of a ^{3}He atom in liquid ^{4}He via path integrals. A single ^{3}He atom should behave [3] as a well-defined quasiparticle with a two-parameter excitation spectrum $\epsilon(p) = \epsilon_0 + p^2/2m^*$. Under this assumption one can show that the parameter m^* is related, at low temperature, to the long imaginary-time diffusion of the ^{3}He particle in configuration space, along a many-body path. More precisely,

$$\frac{1}{m^*} = 2 \lim_{\beta\to\infty} \langle \{\mathbf{r}(\beta/2) - \mathbf{r}(0)\}^2 \rangle / \beta\hbar^2 , \qquad (3)$$

where $\mathbf{r}(0)$, $\mathbf{r}(\beta/2)$ are the positions of the ^{3}He particle at the initial and middle slices of the many-particle path and the average $\langle \cdots \rangle$ is taken over all paths. We computed m^*, as given by (3) at the two temperatures $T = 0.25$ and 1 K, and observed no significant temperature dependence, within statistical uncertainties; we found $m^*/m = 2.3 \pm 0.1$, in agreement with experiments [6].

The results discussed so far pertain to the $x \to 0$ limit; we now address the question of the investigation of the phase diagram of the isotopic liquid helium mixture. As previously mentioned, below a temperature of about 0.87 K, the mixture is experimentally observed to separate into two coexisting phases, rich in one of the two isotopes. To study this effect quantitatively, we performed an RPIMC simulation of a mixture made of equal fractions of ^{4}He and unpolarized ^{3}He, for a total of 108 particles, at a density of 0.0191 Å^{-3}, equal to the average between the equilibrium density of the two isotopes. The simulation box was chosen to be the set of points (x, y, z) such that $0 \le x, y \le L$, $0 \le z \le 2L$, i.e., a rectangular parallelepiped, with periodic boundary conditions, with L approximately equal to 14 Å. We initially separated the isotopes; i.e., all ^{3}He atoms were located in the region $0 \le z \le L$, whereas ^{4}He atoms were in the region $L \le z \le 2L$. Then, as the simulation proceeded, the particles were allowed to mix. We ran the simulation for a sufficiently long time until a situation characterized by stable density profiles of the two isotopes in the z direction was reached [13].

Our results are shown in Fig. 2, where we compare the density profile in the z direction for ^{3}He, $\rho_3(z)$, and ^{4}He, $\rho_4(z)$, at the two temperatures which we considered, i.e., 250 and 500 mK, and at saturated vapor pressure. As a first comment, we note that even at the higher of the two temperatures, where considerable mixing occurs and where finite-size effects are more important due to the proximity to the critical point, two separate phases are nonetheless clearly identifiable, in remarkable qualitative agreement with experimental observation, despite the relatively limited size of the system studied and the RPIMC nodal approximation. Let us indicate by ρ_A^M the peak value of the density of the isotope ^{A}He in the ^{A}He-rich phase region, and by ρ_A^m its lowest density in the ^{B}He-rich phase region. At $T = 250$ mK ρ_3^M and ρ_4^M are within 10% of the equilibrium density values (dashed line in Fig. 2); on assuming that ρ_A^m and ρ_B^m approximate reasonably well the asymptotic values in the bulk mixtures, we can estimate the solubility χ_A of ^{A}He in ^{B}He

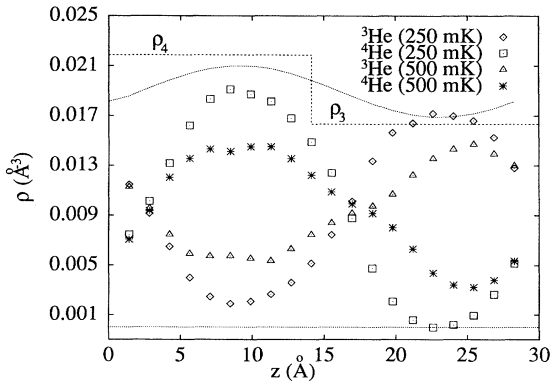

FIG. 2. Equilibrium density profiles $\rho_3(z)$ for ^{3}He and $\rho_4(z)$ ^{4}He in the z direction of the simulation box, at $T = 500$ and 250 mK. The dotted line represents the total density $\rho(z) = \rho_3(z) + \rho_4(z)$ at $T = 250$ mK, which looks very similar at $T = 500$ mK. The dashed line represents the equilibrium density of pure ^{4}He (ρ_4) and of pure ^{3}He (ρ_3). Statistical errors (one standard deviation) are smaller than the sizes of the symbols.

as $\rho_A^m/(\rho_A^m + \rho_B^M)$; the results are reported in Table II. The estimates at $T = 250$ mK are in excellent agreement with experimental determinations [2,12], whereas at $T = 500$ mK the solubilities are overestimated, presumably due to finite-size effects.

At $T = 250$ mK an interface between the two phases appears well defined; its location is at $z \approx 3$ and 16 Å and its width w, defined as the length of the z interval in which $0.1\rho_A^M + 0.9\rho_A^m \leq \rho_A(z) \leq 0.9\rho_A^M + 0.1\rho_A^m$, is of the order of 10 Å. As ground state Monte Carlo calculations for a free ^{4}He surface show [14], the interfacial width is considerably reduced by the finite size of the simulation box; thus, in the limit in which the size of the box along the z direction becomes very large, we can expect the interfacial width to be greater than 10 Å, i.e., significantly larger than the width of a liquid ^{4}He free surface, which is about 4–5 Å, as experimentally measured by ^{4}He scattering [15]. For a large surface, the interfacial width is not well defined, due to roughening caused by long-wavelength ripplons; however, it is meaningful for finite systems in confined geometries, where long-wavelength ripplons are suppressed.

This suggests a possible interpretation of a recent, intriguing experiment [16] in which an isotopic liquid helium mixture was placed inside highly porous silica aerogel, which forms an essentially random network of interconnected strands of diameter of about 30 Å. In this experimental setting, superfluidity was detected at a ^{4}He concentration as low as 4%, at a temperature of the order of 0.3 K, thus well above the ^{3}He superfluid transition temperature, which is in the mK range. Kim, Ma, and Chan argue that this surprising result could be explained in terms of an enhanced ^{4}He solubility in ^{3}He, caused in some fashion by the microstructure of the silica aerogel network [16].

Our results indicate that a simpler picture can be considered. At low ^{4}He concentrations ^{4}He atoms, which have a greater mass and therefore can bind more effectively to aerogel, adhere to the randomly distributed aerogel strands, forming isolated ^{4}He "domains." In the absence of ^{3}He, ^{4}He superfluidity is confined to these domains, i.e., to the ^{4}He-coated surfaces of the silica strands; the presence of ^{3}He, on the other hand, increases the effective thickness of the ^{4}He film coating the strands with respect to what it would be if ^{3}He were absent, thereby greatly enhancing the tunneling rate of ^{4}He atoms between separate ^{4}He domains. This can establish phase coherence and give rise to superfluidity throughout the sample. In other words, there is no greater solubility of ^{4}He in ^{3}He in aerogel, but simply a larger fraction of the system consists of a ^{4}He-^{3}He interfacial region. More work will be needed to establish this conclusion more quantitatively, including a systematic investigation of finite-size effects as well as of the sensitivity of the results upon changes in the trial nodal regions; however, the results presented in this work show how the PIMC formalism provides an effective framework to investigate quantitatively this type of phenomena.

TABLE II. Solubility of ^{3}He in ^{4}He (χ_3) and of ^{4}He in ^{3}He (χ_4), deduced by the density profiles of Fig. 2. Fourth and fifth columns report experimental results. The total number of particles is $N = 108$, half for each isotope. Statistical errors (one standard deviation), in parentheses, are on the last digit.

T (mK)	χ_3	χ_4	χ_3(exp)	χ_4(exp)
250	0.09(1)	0.00(1)	0.10	0.00(1)
500	0.27(2)	0.18(2)	0.22(1)	0.09(1)

This work was supported by the Office of Naval Research under Contract No. N00014-J-92-1320 and by the National Center for Supercomputing Applications (NCSA).

[1] J. Bardeen, G. Baym, and D. Pines, Phys. Rev. Lett. **17**, 372 (1966).
[2] E. H. Graf, D. M. Lee, and J. D. Reppy, Phys. Rev. Lett. **19**, 417 (1967); C. Ebner and D. O. Edwards, Phys. Rep. **2C**, 77 (1971).
[3] L. D. Landau and I. Pomeranchuk, Dokl. Nauk SSSR **59**, 669 (1948).
[4] W.-K. Lee and B. Goodman, Phys. Rev. B **24**, 2515 (1981); J. Boronat, A. Polls, and A. Fabrocini, J. Low Temp. Phys. **91**, 275 (1993).
[5] J. C. Owen, Phys. Rev. B **23**, 5815 (1981).
[6] R. A. Sherlock and D. O. Edwards, Phys. Rev. A **8**, 2744 (1973).
[7] Y. Wang and P. E. Sokol, Phys. Rev. Lett. **72**, 1040 (1994).
[8] R. A. Aziz, M. J. Slaman, A. Koide, A. R. Allnatt, and W. J. Meath, Mol. Phys. **77**, 321 (1992); K. W. Herwig, P. E. Sokol, T. R. Sosnick, W. M. Snow, and R. C. Blasdell, Phys. Rev. B **41**, 103 (1990); for a review on helium interatomic potentials, see R. A. Aziz, in *Inert Gases,* edited by M. L. Klein (Springer-Verlag, Berlin, 1984).
[9] D. M. Ceperley and E. L. Pollock, Phys. Rev. Lett. **56**, 351 (1986); in *Monte Carlo Methods in Theoretical Physics,* edited by S. Caracciolo and A. Fabrocini (ETS Publishing, Pisa, 1991).
[10] D. M. Ceperley, J. Stat. Phys. **63**, 1237 (1991).
[11] D. M. Ceperley, Phys. Rev. Lett. **69**, 331 (1992).
[12] S. Yorozu, M. Hiroi, H. Fukuyama, H. Akimoto, H. Ishimoto, and S. Ogawa, Phys. Rev. B **45**, 12942 (1992).
[13] Translational symmetry requires the density profiles to be uniform; therefore, in order to break the symmetry we defined the origin of the coordinates with reference to the ^{4}He center of mass position.
[14] J. L. Vallés and K. E. Schmidt, Phys. Rev. B **38**, 2879 (1994).
[15] P. M. Echenique and J. B. Pendry, Phys. Rev. Lett. **37**, 561 (1976); V. U. Nayak, D. O. Edwards, and N. Masuhara, *ibid.* **50**, 990 (1983).
[16] S. B. Kim, J. Ma, and M. H. W. Chan, Phys. Rev. Lett. **71**, 2268 (1993).